

Seismic performance assessment of R.C. bridge piers designed with the Algerian seismic bridges regulation

Fouad Kehila^{*}, Abderrahmane Kibboua^a, Hakim Bechtoula^b and Mustapha Remki^c

Department of Civil Engineering, National Earthquake Engineering Research Center CGS,
01 Rue Kaddour RAHIM, BP 252, Hussein Dey, Algiers, Algeria

(Received February 18, 2018, Revised October 4, 2018, Accepted November 23, 2018)

Abstract. Many bridges in Algeria were constructed without taking into account the seismic effect in the design. The implantation of a new regulation code RPOA-2008 requires a higher reinforcement ratio than with the seismic coefficient method, which is a common feature of the existing bridges. For better perception of the performance bridge piers and evaluation of the risk assessment of existing bridges, fragility analysis is an interesting tool to assess the vulnerability study of these structures. This paper presents a comparative performance of bridge piers designed with the seismic coefficient method and the new RPOA-2008. The performances of the designed bridge piers are assessed using thirty ground motion records and incremental dynamic analysis. Fragility curves for the bridge piers are plotted using probabilistic seismic demand model to perform the seismic vulnerability analysis. The impact of changing the reinforcement strength on the seismic behavior of the designed bridge piers is checked by fragility analysis. The fragility results reveal that the probability of damage with the RPOA-2008 is less and perform well comparing to the conventional design pier.

Keywords: fragility curves; seismic performance; damage states; vulnerability; pier bridge

1. Introduction

In Algeria, the road transportation system has a very important consistency which amounts to about 65000 km of roads and covers a vast extent of the national territory. The continuity of this transportation system is maintained by constructing bridges over lakes, tunnels and rivers. Algeria has nearly 6000 road bridges spread across the country, most of them are located in medium to high seismicity zones.

In 1981, the first Algerian seismic design regulation for buildings has been created after the 1980 El Asman destructive earthquake with a magnitude of 7.2, but bridges and roadways structures still designed according to the seismic coefficient method.

Before the implantation of Algerian seismic regulation code for bridge structures (RPOA-2008) in 2010, bridge piers have been designed using the seismic design coefficient method. In this respect, seismic coefficients equal to 10% of the total weight in the horizontal direction and 7% of the total weight in the vertical direction have been used to design these structures. Therefore, most of the

bridges in the Algerian road system do not comply with the new seismic requirements in terms of safety and seismic performance.

Before the application of the new Algerian seismic design code RPOA 2008, the longitudinal reinforcement of bridges, piers was calculated according to the French regulation BAEL 91 Version 99 (Béton Armé aux Etats Limites). The design action effects (bending moment and axial force) were applied at the section of pier with, design combination of the BAEL 91 Version 99. In the case of the RPOA 2008, the bridge pier longitudinal reinforcement is calculated using a combination of live load, dead load and the effect of the seismic load at the same time.

As an example, and according to RPOA 2008, Paragraph 7.2.2.1, the maximum amount of longitudinal reinforcement for reinforced concrete sections in bridge piers is estimated following this equation:

$$0.25\% \leq \frac{A_s}{B} \leq 1.5\% \quad \text{in zone III (High seismic zone)}$$

With: B is the cross-sectional area of concrete

A_s is the longitudinal steel reinforcement area

In the old regulation, diameter and area of the transverse reinforcement given by BAEL 91 (version 99) were calculated using the following equations.

- For the transverse reinforcement diameter

$$\phi_t \leq \min\left(\frac{h}{35}, \frac{b_0}{10}, \phi_l\right) \quad (1)$$

Where:

h : is the height of the section

b_0 : is the width of the section

ϕ_l : is the diameter of the longitudinal reinforcing

- For the distance between stirrups/hoops:

*Corresponding author, Ph.D.

E-mail: fkehila@cgs-dz.org, fouad.kehila@gmail.com

^aPh.D.

E-mail: akibboua@cgs-dz.org

^bPh.D.

E-mail: bechhakim@gmail.com

^cPh.D.

E-mail: mremki@cgs-dz.org

$$S_t \leq \min(0.9d; 40cm) \quad (2)$$

With “ d ” is the effective depth of the cross section
 • For the amount of the transverse reinforcement

$$\frac{S_t}{A_t} \leq \frac{f_e}{0.4b_0} \quad (3)$$

Where “ f_e ” is the yield tensile strength of the transverse reinforcement.

In the new code RPOA 2008, the amounts of the transverse reinforcement as well as the distance between the stirrups/hoops are given in section 7.2.2.2 of the code and which are summarized briefly hereafter.

• For the distance between stirrups/hoops

$$S_t = \min(24\phi_t; 8\phi_t; 0.25d) \quad (4)$$

With: “ ϕ_t ” is the diameter of the transverse reinforcement and “ ϕ_l ” is the diameter of the longitudinal reinforcing bar

• For the amount of the transverse reinforcement

$$\frac{A_t}{S_t(m)} \geq \frac{A_l}{1.6} \frac{f_{el}}{f_{et}} \quad (5)$$

Where:

S_t : is the distance between stirrups/hoops in m

A_t : is the area of longitudinal reinforcement

f_{el} , f_{et} : yield strength of the longitudinal and transverse reinforcing, respectively.

From the past earthquakes in Algeria, neither bridge damages nor their performances have been reported during the previous earthquakes that have struck the country, aside from those observed during the 2003 Zemmouri earthquake (Kibboua *et al.* 2011) with a magnitude of 6.8. The most significant bridge damages were due to the superstructure moving off their bearings and dropping onto the bents caps, columns damage observed in old bridges, shear key at some metallic girders, superstructure rotation, vertical movement, girder movement and buckling as well as some damage at seat-type abutment and to bin-type wing wall (ASCE 2004).

Updating the seismic design made many of the existing bridges not to meet the current seismic standard. As a result, a number of them are characterized by insufficient earthquake safety according to current criteria. To prevent the collapse of those bridges in case of the occurrence of future earthquakes, these structures need to be strengthened or worst case demolished. Therefore, a huge amount of bridge rehabilitation and replacement work need to be done in the near future in Algeria in order to ensure a safe and continuous transportation facility.

In recent years, seismic vulnerability studies of strategic buildings in Algeria were conducted by many researchers (Mehani *et al.* 2011, Remki *et al.* 2016) to predict the nonlinear dynamic response of reinforced concrete and masonry structures. However, some very limited studies concerning the seismic vulnerability of bridges have been developed in Algeria, except the study of (Kibboua *et al.* 2011). In their study, the authors developed fragility curves considering four typical RC bridge piers, they found that cross-sectional geometry and longitudinal reinforcement significantly affects the vulnerability of bridge piers. They concluded that bridges supported on wall piers have a lower

probability of damage than the others. Another study conducted by Kehila *et al.* (2017), they noticed that the developed fragility curves indicate that the Algerian bridges behaved well during seismic events. Therefore, it is necessary to increase these studies in order to compile a database of fragility curves that can help in decision making inspection, maintenance or rehabilitation process.

In order to be able to identify the performance of these bridges, a simple procedure has been developed, through the fragility curves, which is a probabilistic tool that describes the probability of a structure being damaged beyond a certain damage level for a given ground motion intensity level (Billah and Alam 2013, Billah and Alam 2015). They described also the probability of exceeding different limit states (such as damage levels) and can be determined by different methods, such as (experimental, empirical and numerical).

Experimental fragility curves are those developed in which the expected level of damage for a given ground motion intensity is based on the response from shaking table test. Until now, a few studies were developed (Banerjee and Chi 2013, Zhang *et al.* 2016) using experimental fragility curves.

Empirical fragility curves are developed using damage distributions from the post-earthquake field observations or reconnaissance reports (Gardoni *et al.* 2002).

The derived fragility curves are the best way to know the vulnerability of the bridge structures when it is not possible to get neither actual value of the structural damage due to the lack of information from past earthquake, nor ground motion data, analytical fragility curves become necessary to evaluate the vulnerability of bridges.

From the past reviewed works, different analytical methods were used to develop the fragility curves for different types of bridges such as elastic spectral analysis (Hwang *et al.* 2000), Probabilistic Seismic Demand Model (PSDM) using a Bayesian approach (Gardoni *et al.* 2002, Gardoni *et al.* 2003), nonlinear static analysis (Banerjee and Shinozuka 2007, Moschonas *et al.* 2009) or linear/nonlinear time history analysis (NLTHA) (Bhuiyan and Alam 2012, Mosleh *et al.* 2016, Ramanathan *et al.* 2012, Tavares *et al.* 2012) and incremental dynamic analysis (IDA) (Stefanidou and Kappos 2017, Alam and Bhuiyan 2012, Bayat and Daneshjoo 2015).

The main objective of this paper is to evaluate the performance of an old and newly designed bridge pier which is a representative of the most common existing bridges found on the highway system in Algeria. Moreover, the impact of changing reinforcement ratio on the designed bridge piers is checked by fragility analysis.

For this purpose, a seismic performance of bridge piers, for Algerian highways bridge designed with an old static procedure, based on the seismic coefficient method and the new seismic design code for bridges (RPOA-2008), was carried out using the fragility curves. To derive these curves, static pushover analyses and non-linear time history analyses were performed to assess the responses of the designed bridge piers. Incremental dynamic analyses (IDA) for thirty ground motion were carried out to plot the IDA responses for maximum hazard level, and the results were compared for the designed bridge piers. It is important to

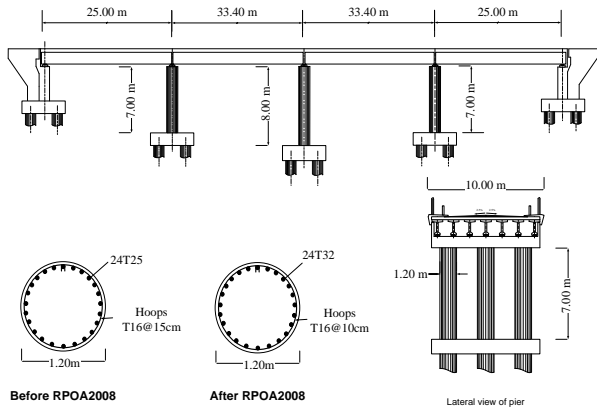


Fig. 1 Longitudinal and lateral views of the bridge and cross-section of the piers

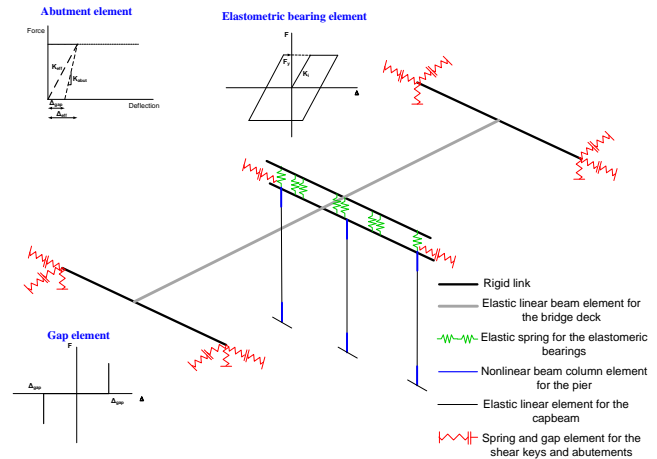


Fig. 2 Numerical model of the bridge

understand how these changes in design affect the dynamic response of a bridge pier and what reinforcement steel can offer in improving bridge performance. Analytical fragility analyses of the designed bridge piers are done by developing probabilistic seismic demand models PSDM. Fragilities were plotted in terms of maximum drift in bridge piers for four different damage states (slight, moderate, extensive and collapse) to predict the performance of the bridge piers under varying ground motion intensities

2. Bridge description

A typical structural bridge pier in Algeria has been selected for the fragility analysis. The bridge is a regular four-span (25+33.4+33.4+25 m) continuous highway bridge with an overall length of 116.80 m. It consists of a reinforced concrete (RC) deck- girder system isolated by rubber bearings installed below the concrete girder supported on top of RC pier cap. The superstructure consists of a longitudinally reinforced concrete deck slab of 10 m wide and it is supported by three sets of piers and by an abutment at each end. The piers have circular cross sections of diameter equal to 1.20 m and heights equal to 7 m and 8 m (the pier of 7m was used in our assessment). The girder cross-section of the bridge model is shown in Fig. 1. Bridge piers were designed based on the old Algerian design provisions (before 2008) called “the seismic coefficient method” where 10% of the total weight in the horizontal direction and 7% of the total weight in the vertical direction are taken as loads due to the seismic effect.

3. Numerical model

To conduct nonlinear time history analyses, a three-dimensional analytical model of a bridge pier was generated in SeismoStruct (SeismoSoft 2016) software. Circular pier section was modelled with fiber beam-column, each fiber has a stress-strain relationship, which can be specified to represent unconfined concrete, confined concrete, and longitudinal steel reinforcement. Elastic frame element was

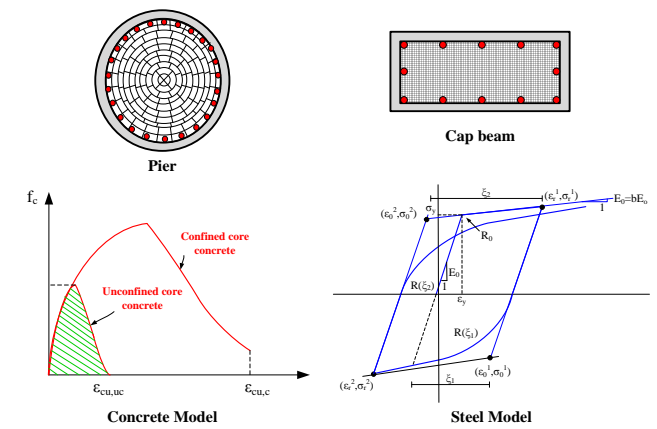


Fig. 3 Fiber-based discretization

used to model the deck and girders with the cross-sectional properties, flexural (EI) and shear rigidity (GJ). A bilinear symmetric zero length link element was used to define the elastomeric bearing in the longitudinal and transverse direction and was connected with girder using rigid links. Three translational and three rotational linear spring elements were used to define the spring and dashpot elements to characterize the active and passive action of the seat type abutment. The abutment was modelled with a model proposed by Aviram *et al.* (2008). The gap between deck and abutment was modelled using a linear gap/hook element defined in SeismoStruct (SeismoSoft 2016). Elastomeric bearing, gap element and abutment link element were connected in series to model the longitudinal response of the bridge. Fig. 2 shows the numerical 3-D analytical model of the selected bridge representative of a common type of existing bridges in Algeria.

3.1 Bridge pier model

The Seismostruct software has been used for the nonlinear finite element modelling of a single column circular bridge pier. This software had been used by researchers to model bridges and bridge components very efficiently (Billah *et al.* 2015, Fakharifar *et al.* 2015a). Fiber element approach was employed, see Fig. 3, to

represent the distribution of inelasticity along the length and cross-sectional area of the member. The fiber section used for the column was discretized into confined concrete, unconfined concrete and steel fiber for reinforcement bars. The concrete model was defined using the constitutive relationship proposed by Mander *et al.* (1988). To simulate the behavior of steel reinforcement, the steel model proposed by Menegotto and Pinto (1973) with isotropic hardening rules defined by Filippou *et al.* (1983) were used in the modelling.

If an elastic system is subjected to large displacements, the geometric nonlinearity has to be taken into account because the displacements are no more proportional to the applied loads.

This kind of nonlinearity is taken into account by introducing a 'co-rotational formulation' as described by Correia and Virtuoso (2006), that refers to the provision of a single element frame that continuously rotates with the element. Since in large displacements the dominant motion is due to the rigid motion, if this one is eliminated, the elastic deformation can be isolated. For this reason, a local reference system (local chord system) is attached to each finite element and it translates and rotates with the element in order to describe the current unknown deformation; finally, a transformation from the local to the global reference system gives the final global response of the system.

In SeismoStruct software, the local and global geometric nonlinearities are automatically taken into account by the program during the analysis. The large displacements and rotations effects are modelled considering the co-rotational formulation and the beam-column effects considering a cubic formulation that computes the transverse displacement as a function of the end-rotations of the element.

3.2 Validation of the numerical model

In order to validate the numerical model used in our study, the software SeismoStruct has been used to verify the efficacy of the program, a circular bridge column from (Takemura and Kawashima 1997) was selected to catch the strength, deformation and stiffness transition under reversed cyclic loading

For this purpose, a 400-mm diameter circular column for cyclic loading (Takemura and Kawashima 1997) was analyzed. The effective height of the column was 1350 mm. The compressive strength of concrete and yield strength of the longitudinal reinforcement were 30 MPa and 374 MPa respectively. Thirteen D16 (16 mm diameter) longitudinal reinforcements were used in the column as shown in Fig. 4(b). Tie bar of 6 mm diameter with a yield strength of 363 MPa was used. Constant axial load of 185 kN was applied during the loading history. Displacement control using the cyclic loading shown in Fig. 4(a) was used. The loading was applied at 1450 mm from column base.

Fig. 4(b) shows a comparison between the experimental and the analytical hysteretic curves of the circular RC column. Obtained results from the analytical modelling show that the SeismoStruct software can predict the performance of the specimen with a good accuracy. In our

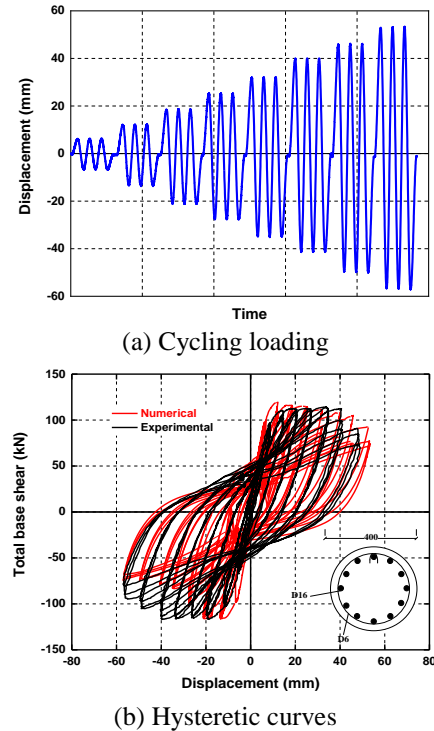


Fig. 4 Numerical and experimental results

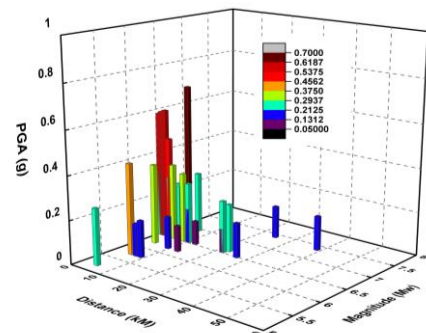


Fig. 5 Distribution of PGA related to magnitudes and epicentral distance

case, the difference between the numerical and the experimental results was only 4.17% for the maximum shear capacity and 6.78% for the dissipated energy.

The obtained results illustrate the effectiveness of the program in predicting the seismic performance of a reinforced concrete bridge pier for a wide range of material properties.

4. Ground motion selection

To take into account the importance of various characteristics of the input ground motion such as duration, frequency contents, phase, site type...etc. on the performance of the bridge, 30 real records varying from weak to strong probabilistic intensities were used as input excitation to examine the seismic behavior of the bridge to different excitation levels (Catalan *et al.* 2010, Marra *et al.* 2017, Vamvatsikos and Cornell 2002), see Table 1. These

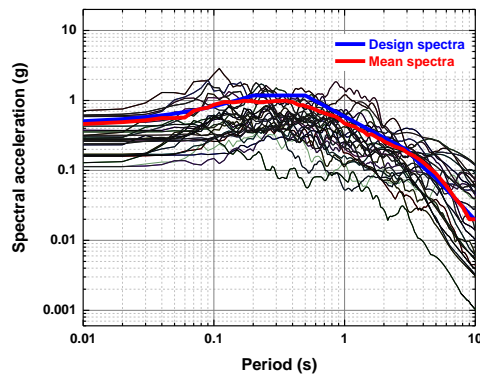


Fig. 6 Acceleration response spectra for the different suits of ground motions

ground motions used in this paper were chosen from the Pacific Earthquake Engineering Research Center (PEER) Strong Motion Database, and have low to medium values of PGA, R , M_w and PGV, which are in the range of 0.052-0.70 g, 0.35-38.89 km, 5.2-7.4 and 4.3-151.15 cm/sec, respectively. The soil conditions correspond to an average shear wave velocity (V_s) ranging between 200 m/s and 400 m/s at 30 m depth. The distribution of peak ground accelerations (PGA's) related to magnitudes (M_w) and epicentral distance (R) is shown in Fig. 5.

All ground motions are taken into consideration to generate sufficient data to plot fragility curves. The ground motion records are scaled to the design spectrum of the region for 5% damping ratio of soft soil type S3 with the SeismoMatch (SeismoSoft 2016) software. Fig. 6 shows the response spectra for the different suits of ground motions.

5. Limit states

Limit states are defined on different types of engineering demand parameter such as bridge pier ductility, pier displacement, isolation bearing displacement, bearing shear strain percentage, pile displacement, and abutment displacement. HAZUS-MH (FEMA 2003) defined four limit states (slight, moderate, extensive and collapse), which are most commonly used in seismic fragility analysis.

FEMA (FEMA 2003) specified onset of cracking in concrete cover and minor spalling as slight damage in bridge pier. Yielding defines the moderate damage state, which can also be described by physical phenomenon of moderate cracking and minor spalling in concrete. Extensive damage with degradation can be captured by spalling of concrete and crushing of confined core concrete may lead to the probable collapse of the bridge pier. Priestley *et al.* (1996) suggested that the cracking and spalling of cover concrete occur at 0.0014 and 0.004 strain.

Table 1 Characteristic of selected ground motions

EQ. N ^o	M_w	Year	Earthquake name	Earthquake record station	R (Km)	PGA (g)	PGV (cm/s)
1	6.95	1940	Imperial Valley-02	El Centro Array #9	6.09	0.28	30.94
2	7.36	1952	Kern County	Taft Lincoln School	38.89	0.16	15.23
3	6.5	1954	Northern Calif-03	Ferndale City Hall	27.02	0.16	72.14
4	6.19	1966	Parkfield	Cholame - Shandon Array #5	9.58	0.15	7.10
5	6.19	1966	Parkfield	Cholame - Shandon Array #8	12.9	0.12	4.30
6	6.61	1971	San Fernando	LA - Hollywood Stor FF	22.77	0.22	21.72
7	6.24	1972	Managua, Nicaragua-01	Managua, ESSO	4.06	0.37	58.12
8	5.2	1972	Managua, Nicaragua-02	Managua, ESSO	4.98	0.26	50.81
9	6.8	1976	Gazli, USSR	Karakyr	5.46	0.70	100.33
10	5.74	1979	Coyote Lake	Gilroy Array #2	9.02	0.17	13.70
11	5.74	1979	Coyote Lake	Gilroy Array #3	7.42	0.15	14.36
12	5.74	1979	Coyote Lake	Gilroy Array #4	5.7	0.42	30.57
13	6.53	1979	Imperial Valley-06	Aeropuerto Mexicali	0.34	0.31	42.79
14	6.53	1979	Imperial Valley-06	Agrarias	0.65	0.29	34.93
15	6.53	1979	Imperial Valley-06	Bonds Corner	2.66	0.6	93.50
16	6.53	1979	Imperial Valley-06	Brawley Airport	10.42	0.16	73.21
17	6.53	1979	Imperial Valley-06	Calexico Fire Station	10.45	0.28	44.91
18	6.53	1979	Imperial Valley-06	Chihuahua	7.29	0.27	24.80
19	6.53	1979	Imperial Valley-06	Delta	22.03	0.24	26.33
20	6.53	1979	Imperial Valley-06	El Centro - Meloland Geot. Array	8.6	0.32	145.88
21	6.53	1979	Imperial Valley-06	El Centro Array #10	21.98	0.11	18.18
22	6.53	1979	Imperial Valley-06	El Centro Array #13	7.05	0.05	7.1
23	6.53	1979	Imperial Valley-06	El Centro Array #4	3.95	0.29	33.73
24	6.53	1979	Imperial Valley-06	El Centro Array #5	1.35	0.59	79.07
25	6.53	1979	Imperial Valley-06	El Centro Array #7	0.56	0.58	54.14
26	6.53	1979	Imperial Valley-06	El Centro Array #8	3.86	0.47	47.17
27	6.53	1979	Imperial Valley-06	El Centro Differential Array	5.09	0.35	151.15
28	6.53	1979	Imperial Valley-06	Holtville Post Office	7.5	0.26	106.27
29	6.53	1979	Imperial Valley-06	Parachute Test Site	12.69	0.11	36.55
30	7.4	1971	San Fernando	Santa Felita Dam	24.87	0.15	10.74

Table 2 Comparison between IDA and SPA results

Pier	Yielding displacement (mm)		Crushing displacement (mm)	
	Median IDA	SPA	Median IDA	SPA
Before	49.8	47.6	264.5	258.3
After	55.2	50.4	351.2	343.7

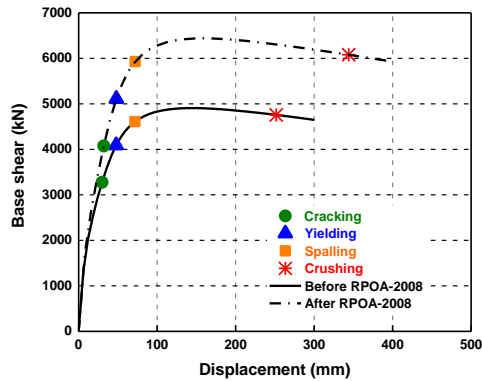


Fig. 7 Limit states from pushover analysis

These suggested values are used in defining slight and extensive damage states. Moderate damage is taken at a displacement when the longitudinal steel rebar yields and collapse in bridge pier is considered at crushing strain of concrete. This performance criterion marks the unsuitability of use of the bridge and requirement of probable replacement. The yield strength of transverse reinforcement considerably affects the crushing strain of concrete.

In this study, limit states are measured from static pushover analysis on bridge pier drift capacity. Static pushover analysis and Time history analyses were carried out for the pier designed before and after the Algerian seismic bridge regulation RPOA-2008 with different percentage of the longitudinal reinforcement in order to assess the performance criteria. These performance criteria are presented in terms of material strain (concrete compressive strain and steel strain for reinforced concrete bridge pier). Non-linear time history analyses are also carried out to check the performance of the bridge piers under seismic motions. The program SeismoStruct (SeismoSoft 2016) can show the material strain levels for stated performance criteria with reasonable accuracy (Billah and Alam 2016b).

Drift percentage at the initiation of cracking, yielding of longitudinal steel, spalling of concrete cover and crushing of core concrete is considered as slight, moderate, extensive and collapse limit states for the bridge piers respectively.

Material strain levels are defined to predict the damages in the bridge piers. The cracking strain of concrete is considered at 0.0014 and the concrete spalling is assumed to occur at a compressive strain of 0.004 as recommended by Priestley *et al.* (1996). Longitudinal rebar yields at 0.0021 strain calculated from the yield strength and elastic modulus of steel.

Paulay and Priestley (1992) suggested the following equation, $\epsilon_{cu} = 0.004 + 1.4 \rho_s f_{yh} \epsilon_{sm} / f'_c$ which is used in defining the crushing strain of concrete, where, ϵ_{sm} is the steel strain at maximum tensile stress (0.12); f'_c = concrete compressive

Table 3 Damage states of bridge piers following FEMA 2003

Limit States	Physical Phenomenon (FEMA, 2003)	Before RPOA- 2008		After RPOA- 2008	
		Displacement (mm)	Drift (%)	Displacement (mm)	Drift (%)
Slight	Cracking and minor spalling	29.4	0.42	32.2	0.46
Moderate	Moderate cracking and spalling	47.6	0.68	50.4	0.72
Extensive	Degradation without collapse	71.4	1.02	73.5	1.05
Collapse	Failure leading to collapse	258.3	3.69	343.7	4.91

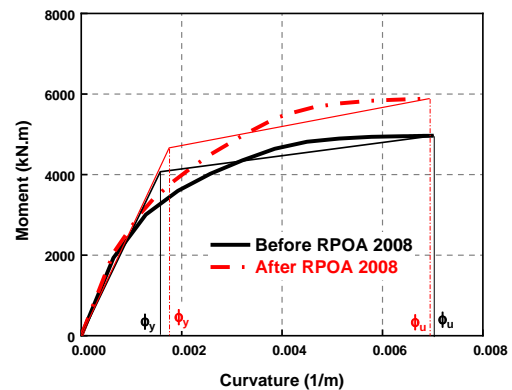


Fig. 8 Moment - curvature curve

strength (27 MPa); f_{yh} = yield strength of transverse steel (400 MPa); and ρ_s is the volumetric ratio of spiral (2.1%). The crushing strain of concrete is found to be 0.053, which exceeds the limit 0.05 founded by Paulay and Priestley (1992).

Fig. 7 shows the different limit states which are shown on the static pushover analysis curve for bridge piers designed before the RPOA-2008 and with RPOA-2008 regulation bridge code.

Yielding in bridge columns happens at a displacement 47.6 mm and 50.4 mm respectively. From the incremental dynamic analysis of the bridge columns, the median values for yield displacement are found 49.8 mm, and 55.2 mm as summarized in Table 2. The variations in yield deformation results from static analysis and IDA are 4.41%, and 8.69% for old and new design piers, respectively. For the case of crushing displacement, the variation becomes 2.34% and 2.13% for old and new design piers, respectively. These small variations confirm the reasonable accuracy of damage state definition from static pushover analysis. Summary of different limit states physical appearance and criteria are presented in Table 3.

6. Moment-curvature relationship

Fig. 8 shows the moment-curvature relationships using the sectional analyses as well as the associate equivalent bilinear curves, respectively, for the pier designed before and after the ROPA-2008. In both cases, the curves show

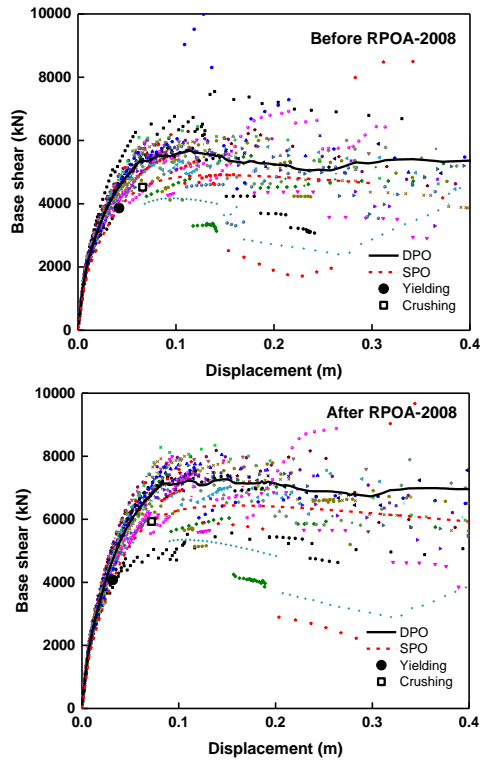


Fig. 9 Comparison of dynamic and static pushover curve before and after the RPOA-2008

almost similar initial stiffness and post-elastic transition. The maximum moment capacities were observed at a curvature of 0.007 (1/m).

7. Static and dynamic pushover curves

Incremental Dynamic Analysis, IDA, was carried out to generate a set of structural response data for increasing intensity level of ground motions. A Dynamic Pushover (DPO) curve was generated by plotting the maximum displacements and the corresponding base shear of the structure.

The Static Pushover (SPO) curves were compared to the DPO curves. Fig. 9 shows the total base shear versus the lateral displacement relationship curves for bridge pier with 7 m in height before and after the RPOA-2008. It can be observed that the dynamic pushover curves DPO are closer to the static pushover curves SPO before the first yield of the longitudinal reinforcements. The DPO curve shows higher base shear capacity compared to the SPO curve between the first yield and first crushing of the concrete, however, the variation of DPO and SPO is within 15.1% for the old design and about 13.43% for the new RPOA-2008. The DPO base shear capacity is higher than that obtained by the SPO curve beyond crushing point.

8. Incremental dynamic analysis IDA

The Incremental Dynamic Analysis, IDA, is generally used to estimate the bridge performance due to seismic

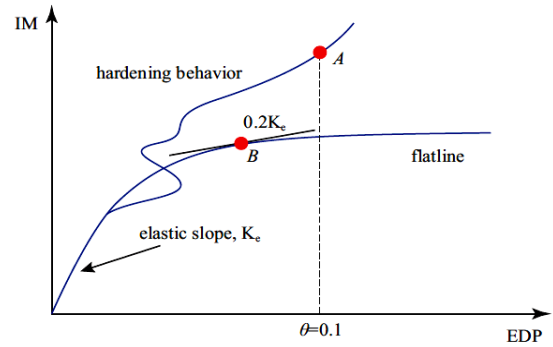


Fig. 10 Collapse of a typical IDA curve

actions (Baker 2015, Billah and Alam 2015, Fakharifar *et al.* 2015b, Chandramohan *et al.* 2016). IDA was first introduced by Luco and Cornell (1998) and widely elaborately by Vamvatsikos and Cornell (2002). Series of non-linear time history analyses were carried out for a given selected ground motion record with increased intensity until the structure becomes unstable or the maximum response of the structure is reached. The IDA was performed for multiple earthquake records to obtain the relationships between the demand and the capacity of the structure. Ground motion intensity levels were selected to cover the whole limits of the structural response from yielding to failure (Billah and Alam 2014).

It is assumed that in the numerical model of the structure employed for IDA, stiffness and strength degradation under dynamic loading are acceptably represented. Consequently, failure of the analysis to provide an EDP value after scaling a record to a certain IM level can be attributed to the onset of dynamic instability, which would physically correspond to the structure collapse. This is usually when convergence is not reached any more.

The IDA curve starts with a straight line in the elastic range, of which the slope is marked by K_e . According to FEMA 350, there are two collapse limit-state rules, i.e., the IM-based rule and EDP-based rule.

The IM-based rule is represented by the point with a slope equal to 20% of the elastic slope on the IDA curve, as shown in Fig. 10. If the drift angle $\theta > 0.1$, then $\theta = 0.1$ according to the EDP-based rule, when the collapse limit state is reached. The idea of the IM-based rule is that with the IM increasing, the EDP is increasing at an even higher rate and may approach 'infinity', which can be regarded as the occurrence of dynamic instability. Numerical instability similar to dynamic instability is often encountered in analyzing the structure near the collapse state, and divergence in iterations may be adopted as an indicator for judging the collapse limit state.

The collapse can be displayed at the end of the IDA curve as a horizontal segment of ever-increasing EDP-values for a fixed IM value.

8.1 PGA versus maximum drift

A suite of thirty ground motion records as shown in Table 1 were used to carry out the IDA in order to determine the maximum drift capacity and yield behavior of

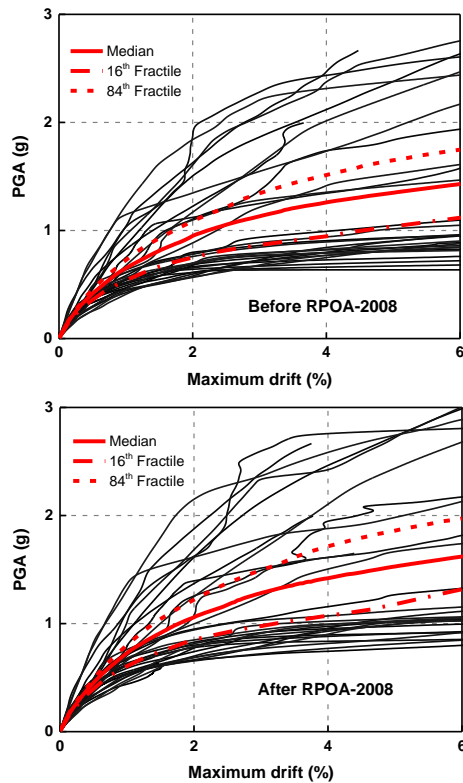


Fig. 11 IDA curves for drift

the bridge piers under dynamic loading. These seismic motions are scaled to match the response spectrum based on site-specific before implementing IDA.

Fig. 11 shows the PGA versus the maximum drift of the bridge pier for individual ground motion records. All the plots show somewhat elastic behavior before starting non-linearity, and scattered curves indicate how the response varies even for the same intensity earthquakes. The diversified frequency content of ground motions can be attributed to such behavior. The pier designed with RPOA-2008 show higher stiffness than the pier designed before the RPOA-2008. Higher reinforcement ratio results in higher stiffness of the structure. However, the inelastic behavior of the bridge piers is quite different with gradual softening towards failure for bridge columns. It can be observed that the pier design before the RPOA-2008 can sustain an earthquake with 2.5 g with a drift of 6%. However, for pier designed with the RPOA-2008, the acceleration is higher than 2.5 g for the same drift. The IDA curves are random lines or function of intensity measures (IM) (Vamvatsikos and Cornell 2002). To understand their comparative performance with more reliable data, the curves are also summarized in terms of 16th, median (50th) and 84th fractile values. Mean, median and 84th fractile values are mostly used in engineering design (Billah and Alam 2014). Fig. 11 displays the developed 16th, median (50th), and 84% fractile curves in terms of maximum drift for distinct ground motion intensities.

For the PGA value of 1 g, 16% ground motion records reached the maximum drift of 1.98%, and 3.91% for the pier designed before and after the seismic design code RPOA-2008, respectively. For the same value of PGA=1 g,

50% of seismic motions reached a maximum drift of 2.26% and 1.78% for the pier designed before and after the Algerian seismic design regulation, RPOA-2008.

Pier designed before RPOA-2008 experienced a drift of 1.69% for 84% of ground motions at PGA of 1 g, whereas, for pier designed with the RPOA-2008, the results showed that the maximum drift was 17.7% less. It can be concluded that the maximum drift of the bridge pier designed with the new RPOA-2008 is lower than that designed with the seismic coefficient method (before RPOA-2008).

Serviceability and damage of bridge piers are classified by several researchers in terms of the maximum experienced drift. As an example, repairable damage is specified between 0.5 and 1.5% drift, and the near collapse between 2, 2.5 and 5% drift (Liu *et al.* 2012, Ghobarah 2001, Kim and Shinozuka 2004, Fakharifar *et al.* 2015b, Liu *et al.* 2012, Ghobarah 2001, Kim and Shinozuka 2004, Fakharifar *et al.* 2015b, Banerjee and Shinozuka 2008).

In this study, the damage is calculated from the pushover analysis. The maximum compressive strain in the confined core concrete and the maximum tensile strain in the longitudinal reinforcing steel were considered as the strain-based limit states (Priestley *et al.* 2007).

When the ground motions reached a probability of 50% of PGA=1 g, the damage is classified “irreparable damage” in bridge piers, whatever the regulations code is used.

In the same way, for the pier designed with the RPOA-2008, the “collapse limit” state is reached when the probability of 50% to get a PGA=1.42 g is satisfied. The pier designed before RPOA-2008 (with the seismic coefficient method) is 12% less in terms of PGA.

9. EDP and IM relationship

For a given Intensity Measure (IM) of seismic motions, the Engineering Demand Parameters (EDP) is determined from the inelastic simulation of structures. For bridge structures, the response can be represented in terms of relevant engineering parameters like pier deformation, drift, residual deformation, abutment displacement, isolation bearing displacement and strain. Maximum drift is the most widely used response parameter in fragility analysis of bridge piers. Whereas, Peak Ground Acceleration (PGA) and the spectral acceleration are the most commonly used intensity measure in seismic fragility analysis (Mackie and Stojadinovic 2004, Nielson and DesRoches 2007a, Shinozuka *et al.* 2003).

In our study, PGA is selected as the intensity measure because; the PGA can be obtained directly from earthquake record databases without any additional information. On the other hand, the spatial distribution of PGA values is easier to be estimated through simple or advanced methods within a seismic hazard study of a specific area.

Another method to determine intensity measures is based on the use of the response spectrum of a ground motion, such as spectral values and spectrum intensity parameters (Donaire-Ávila *et al.* 2015, Beilic *et al.* 2017), which can be calculated by utilizing response spectrum periods, or specific equations, are used for the calculations. Since PGA is one parameter with common applications in

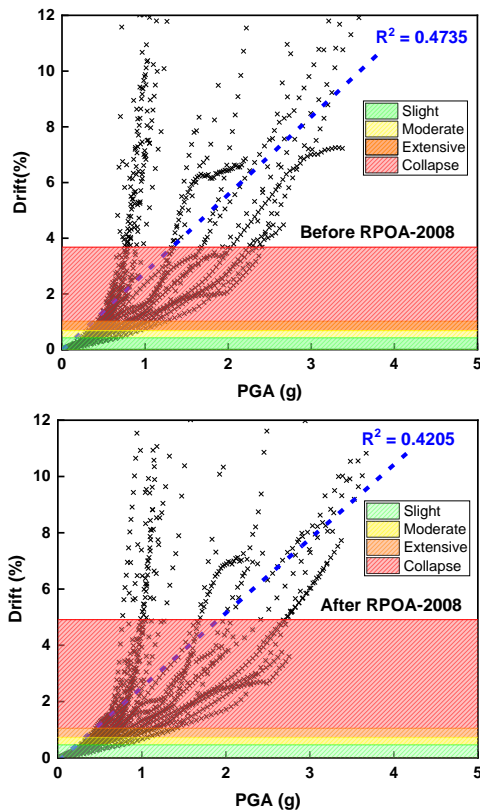


Fig. 12 Drift-PGA relationship

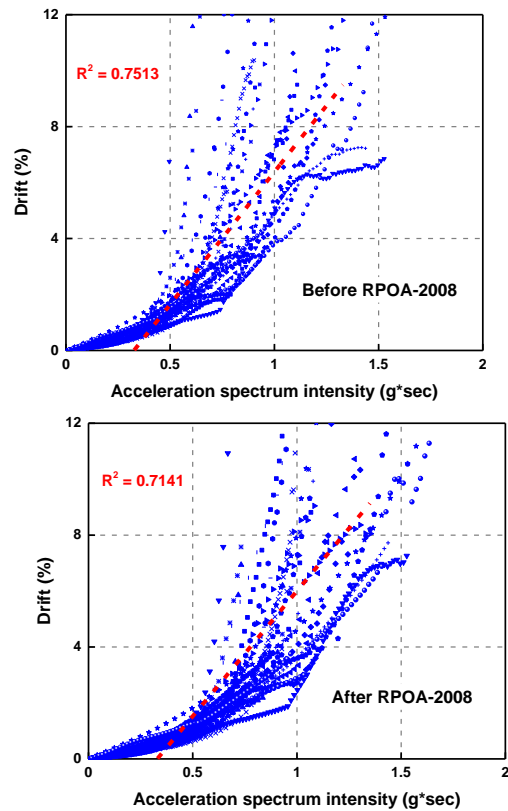


Fig. 13 Drift vs. acceleration spectrum intensity

earthquake engineering. Also, PGA is used by a large number of researchers as the intensity measure to develop fragility curves for bridges.

The bridge community is still predominantly using PGA as the intensity measure. The reason is the difficulty in comparing the fragility of various bridges types. When the bridge types have different fundamental periods, the fragility comparisons must be done at a specific ground motion, why the comparison between fragility curves are easier with a general IM such as PGA.

In this study, PGA is considered as the IM of the ground motions to compare the response of the bridge piers in terms of maximum drift percentage. A new intensity measure IM, such as spectral intensity (SI) are examined and compared to the PGA, in order to understand the variation of EDP with respect to the IM.

9.1 Drift versus PGA

Fig. 12 shows the relationship between the maximum response of bridge piers and the ground motion parameter PGA. As the ground motion intensity increases, the maximum drift of bridge piers increases. These increments do not follow a linear path. Rather, the maximum response becomes scattered, and the dispersion demand increases with the increasing ground motion intensity. The R -squared values are shown in Fig. 12, do not give a good result as for a linear fitting of the drift-PGA relationship. The coefficient of determination, R -squared value, indicates the robustness of the regression. The range of R -squared values from the regression model is 0.47-0.42, for the pier designed before

and after the RPOA-2008, respectively. It can be observed that for a PGA less than 1 g, the small dispersion may allow predicting the response of structure considering a linear variation of EDP and IM.

Logarithmic correlation between PGA and maximum drift are commonly used in developing the probabilistic seismic demand model. (Karamlou and Bocchini 2015, Zhong *et al.* 2016). Colors in Fig. 12 show the limit states for pier designed before and after the RPOA-2008. The colors represent the following damage state: green for slight damage, yellow for moderate damage, orange for extensive damage and red for collapse.

9.2 Drift versus spectrum intensity

The Spectrum Intensity (SI) shows the potential of a ground motion intensity measure in predicting seismic response of soil deposits (Bradley *et al.* 2009). SI of a ground motion was first defined by Housner (1963) as the integral of pseudo-spectral velocity (PSV) from 0.1 to 2.5 sec of the ground motion, the damping ratio of 5% is commonly used to compute the PSV. The correlation between the drift response of the designed bridge piers and the SI as a ground motion measure is shown in Fig. 13. Compared to PGA, SI shows smaller dispersion in demand parameter and maximum drift follows an increasing trend with increased SI. With less amount of longitudinal reinforcement for pier designed before RPOA-2008, the dispersion in demand parameter increases. The R -squared for a linear fitting varied between 0.75 and 0.71 for a pier designed before and after the RPOA-2008, respectively.

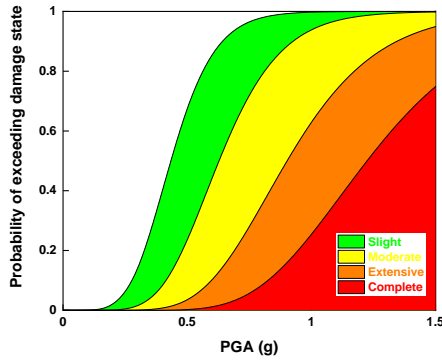


Fig. 14 Fragility curves

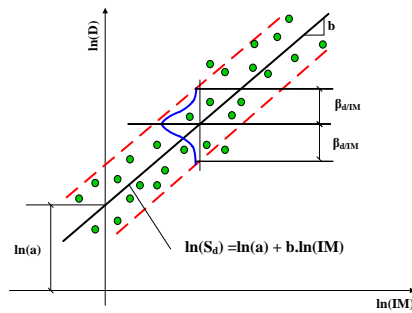


Fig. 15 Illustration of PSDM

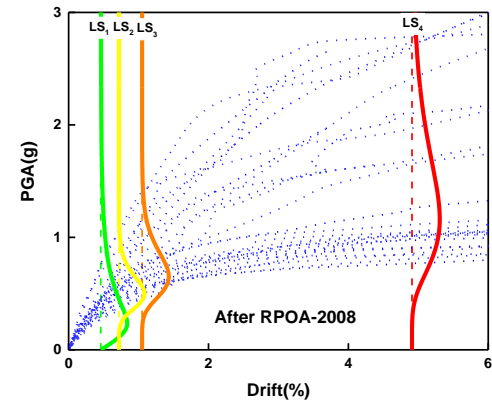
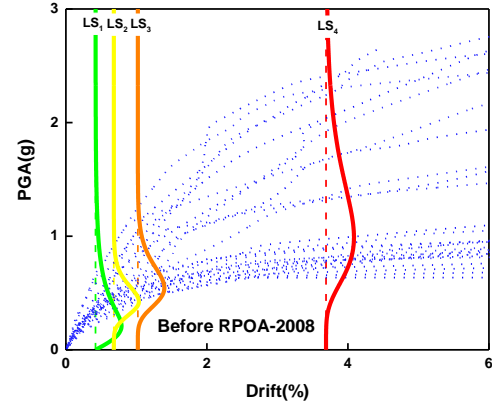


Fig. 16 IDA results with limit states

10. Fragility analysis of the bridge

The PSDM establishes a correlation between the EDPs and the IMs. The PSDM model is regarded as the most rigorous and reliable analytical method to derive fragility functions (Shinozuka *et al.* 2000, Billah *et al.* 2013). The cloud approach (Nielson and DesRoches 2007) was used to develop the PSDM model utilizing the IDA results. Fragility curves were developed for four damage states, namely slight, moderate, extensive and collapse such the one shown in Fig. 14, as an example.

Regression analyses were undertaken to acquire the mean and standard deviation for each damage state, by assuming the power law model, given by Eq. (6), as suggested by Cornell *et al.* (2002), which derives a logarithmic correlation between median EDP and the selected IM, see Fig. 15.

$$\overline{EDP} = a(IM)^b \quad (6)$$

$$\ln(\overline{EDP}) = b \ln(IM) + \ln(a) \quad (7)$$

In Eq. (6), a and b are unknown coefficients which can be estimated from a regression analysis of the response data collected from the nonlinear time history analysis that can be determined using Eq. (7). In order to create sufficient data for the cloud approach, the incremental dynamic analysis is carried out instead of nonlinear time history analysis. The dispersion of the demand, $\beta_{EDP/IM}$, conditional upon the IM can be estimated from Eq. (8).

$$\beta_{EDP/IM} = \sqrt{\frac{\sum_{i=1}^N [\ln(EDP_i) - \ln(a(IM_i)^b)]^2}{N-2}} \quad (8)$$

Fig. 16 shows a comparison between the seismic demands on bridge piers with respect to the different limit states. The LS_1 to LS_4 shown in the figure, corresponds to the slight damage to collapse state. It can be observed that the drift corresponding to the collapsed state, changed for a pier designed before or after the RPOA-2008 from a value of 3.7% to a value of 5%.

Peak responses of the bridge piers in term of drift are considered for the corresponding ground motion intensity to generate the PSDM. The logarithm of drift ratios is plotted in the vertical axis and the logarithm of PGA in the horizontal axis to find the two coefficients " a " and " b " from the regression analysis. PSDM plots are shown in Fig. 17. Dispersion demand, $\beta_{EDP/IM}$ is also found using the regression values. Variations of the R-squared values are very small between the pier designed before and after the RPOA-2008, but the values are close to 1. It indicates a reasonably good correlation between the EDP and the IM.

11. Fragility analyses results and discussion

The probability of damage state (slight, moderate, extensive and collapse damage) with respect to PGA are shown in Fig. 18 for the pier designed before and after the Algerian seismic bridge regulation RPOA-2008.

It can be seen that for all used strong motion records and for a PGA value of 1 g, the probability of slight, moderate, and extensive damage to bridge pier is already 100%. Damage to old designed pier starts earlier than pier designed with the RPOA-2008. At 50% of slight damage

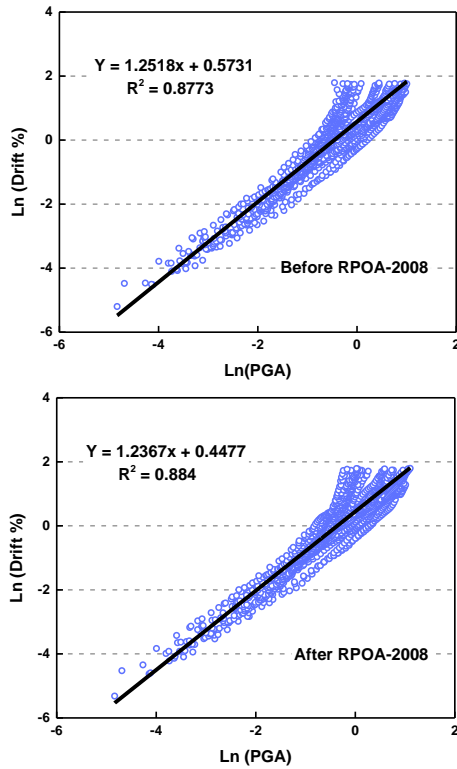


Fig. 17 Probabilistic seismic demand models PSDM

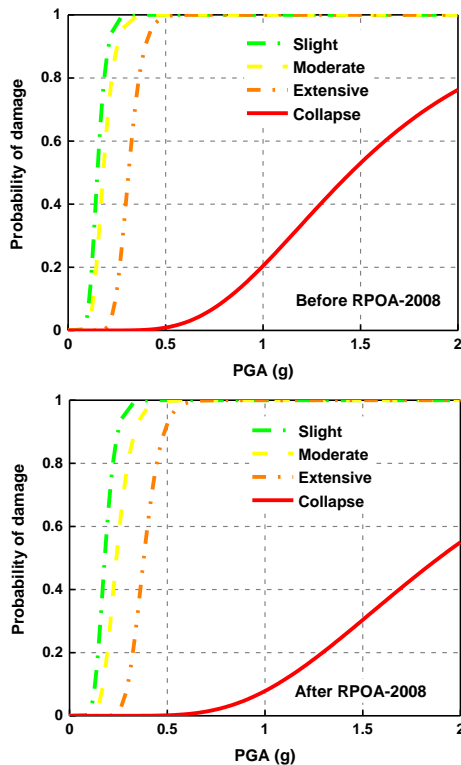


Fig. 18 Fragility curves for pier designed before and after RPOA-2008

probability of the two designed piers, the corresponding PGA values were as low as 0.14 g and 0.17 g, respectively. The same remark can be done for the case of the extensive damage. In this case, the values were, respectively, 0.38 g

Table 4 Fragility performance of the bridge piers

Pier	Damage probability (%)	Slight	Moderate	Extensive	Collapse
		PGA(g)	PGA(g)	PGA(g)	PGA(g)
Before	25	0.12	0.14	0.27	1.06
RPOA-2008	50	0.14	0.17	0.31	1.44
	75	0.18	0.21	0.35	1.96
After	25	0.15	0.21	0.33	1.39
RPOA-2008	50	0.17	0.24	0.38	1.88
	75	0.21	0.28	0.43	2.53

Table 5 Ratios for the PGA variation

Probability (%)	Ratio % (PGA after-PGA before)/PGA after			
	Slight damage	Moderate damage	Extensive damage	Collapse damage
25	20.01	33.33	18.18	23.74
50	17.64	29.17	18.42	23.40
75	14.28	33.33	18.6	22.53

and 0.31 g showing a difference of 18.42%.

The probability of damage to the bridge piers at the collapsed state varied substantially for the case of pier designed before and after the RPOA-2008. At 25% of collapse state probability of the two designed piers, the corresponding PGA values were 1.06 g and 1.39 g, respectively, for piers designed before and after the RPOA-2008, showing a difference of 23.74%.

Steel reinforcement required by the RPOA-2008 did not only increase the stiffness and yield performance of the pier, but the maximum response capacity during dynamic loading also increased leading to higher ductility for the structure. Fragility performances, that show the PGA values that cause 25%, 50% and 75% probability of different damage levels of the bridge piers, are summarized in Table 4.

In Table 5, the ratios between the PGA of the pier designed before and after the RPOA-2008 for different fragility curves states are given.

It is obvious from the previous tables that the damage probability decreases when RPOA-2008 design pier is adopted; especially the collapse performance that was improved significantly. The new Algerian seismic bridge regulation (RPOA-2008) decreased the damage to 17.64, 29.17, 18.42 and 23.40% for slight, moderate, extensive and collapse state at 50% of damage probability.

12. Conclusions

This paper presented the main results of a seismic performance analysis of a typical RC bridge pier designed before and after the Algerian seismic bridge regulation, RPOA-2008. Pier of 7 m height of a four-span continuous highway bridge was selected to assess the seismic performance and to develop the fragility curves.

The numerical model was developed using the Seismostruct software and validated using an experimental database. The model predicted with a good accuracy the performance of the selected piers from the database. In our case, the difference between the numerical and the

experimental results was only 4.17% for the maximum shear capacity and 6.78% for the dissipated energy

Six hundred (600) runs were carried out to assess the responses of the bridge pier of 7 m using Incremental Dynamic Analysis (IDA) method under thirty (30) ground motions that matched to site location design spectrum. Performance limit states were defined from the static pushover analysis curves to generate the fragility curves of the bridge piers in order to improve our understanding of the seismic vulnerability of bridge piers. Two different design alternatives were used in our analysis: seismic coefficient method and the RPOA-2008 regulation.

A Static Pushover analysis, SPO, and Dynamic Pushover analysis, DPO, were compared in this study. The DPO curve shows higher base shear capacity compared to the SPO curve between the first yield and first crushing of the concrete, however, the variation of DPO and SPO is within 15.1% for the seismic coefficient method and about 13.43% for the RPOA-2008.

Comparison between the vulnerability of the pier and the corresponding fragility curves show that the seismic performance of the pier designed with the RPOA-2008 was improved considerably while compared to the results of the pier designed with the old seismic coefficient method. The new Algerian seismic bridge regulation (RPOA-2008) decreased the damage to 17.64, 29.17, 18.42 and 23.40% for slight, moderate, extensive and collapse state at 50% of damage probability.

Acknowledgments

This research was supported by the National Earthquake Engineering Research Center, CGS, Algeria.

References

- Alam, S.M., Bhuiyan, R.M.A. and Billah, A.H.M. (2012), "Seismic Fragility assessment of SMA-Bar restrained multi-span continuous highway bridge isolated by different laminated rubber bearings in medium to strong seismic risk zones", *Bull. Earthq. Eng.*, **10**(6), 1885-1909.
- Aviram, A., Mackie, K.R. and Stojadinovic, B. (2008), "Effect of abutment modeling on the seismic response of bridge structures", *Earthq. Eng. Eng. Vib.*, **7**(4), 395-402.
- Baker, J.W. (2015), "Efficient analytical fragility function fitting using dynamic structural analysis", *Earthq. Spectra*, **31**(1): 579-599.
- Banerjee, S. and Chi, C. (2013), "State-dependent fragility curves of bridges based on vibration measurements", *Prob. Eng. Mech.*, **33**, 116-125.
- Banerjee, S. and Shinozuka, M. (2007), "Nonlinear static procedure for seismic vulnerability assessment of bridges", *Comput. Aid. Civil Infrastr. Eng.*, **22**(4), 293-305.
- Banerjee, S. and Shinozuka, M. (2008), "Mechanistic quantification of RC bridge damage states under earthquake through fragility analysis", *Prob. Eng. Mech.*, **23**(1), 12-22.
- Bayat, M. and Daneshjoo, F. (2015), "Seismic performance of skewed highway bridges using analytical fragility function methodology", *Comput. Concrete*, **16**(5), 723-740.
- Beilic, D., Casotto, C., Nascimbene, R., Cicola, D. and Rodrigues, D. (2017), "Seismic fragility curves of single storey RC precast structures by comparing different Italian codes", *Earthq. Struct.*, **12**(3), 359-374.
- Bhuiyan, R.M.A. and Alam, S.M. (2012), "Seismic vulnerability assessment of a multi-span continuous highway bridge fitted with shape memory alloy bars and laminated rubber bearings", *Earthq. Spectra*, **28**(4), 1379-1404.
- Billah, A., Shahria Alam, M. and Bhuiyan, A.R. (2013), "Fragility analysis of retrofitted multi-column bridge bent subjected to near fault and far field ground motion", *J. Bridge Eng.*, ASCE, **18**(10), 992-1004.
- Billah, A.H.M.M. and Alam, M.S. (2014a), "Seismic performance evaluation of multi-column bridge bents retrofitted with different alternatives using incremental dynamic analysis", *Eng. Struct.*, **62-63**, 105-117.
- Billah, A.H.M.M. and Alam, M.S. (2015), "Seismic fragility assessment of concrete bridge pier reinforced with superelastic Shape Memory Alloy", *Earthq. Spectra*, **31**(3), 1515-1541.
- Billah, A.H.M.M. and Alam, M.S. (2016b), "Plastic hinge length of shape memory alloy (SMA) reinforced concrete bridge pier", *Eng. Struct.*, **117**, 321-331.
- Billah, A.H.M.M., Alam, M.S. and Bhuiyan, A.R. (2013), "Fragility analysis of retrofitted multicolumn bridge bent subjected to near-fault and far-field ground motion", *J. Bridge Eng.*, **18**(10), 992-1004.
- Bradley, B.A., Cubrinovski, M., MacRae, G.A. and Dhakal, R.P. (2009), "Ground-motion prediction equation for SI based on spectral acceleration equations", *Bull. Seismol. Soc. Am.*, **99**(1), 277-285.
- Catalan, A., Benavent-Climent, A. and Cahis, X. (2010), "Selection and scaling of earthquake records in assessment of structures in low-to-moderate seismicity zones", *Soil Dyn. Earthq. Eng.*, **30**(1), 40-49.
- Chandramohan, R., Baker, J.W. and Deierlein, G.G. (2016), "Quantifying the influence of ground motion duration on structural collapse capacity using spectrally equivalent records", *Earthq. Spectra*, **32**(2), 927-950.
- Cornell, A.C., Jalayer, F. and Hamburger, R.O. (2002), "Probabilistic basis for 2000 SAC federal emergency management agency steel moment frame guidelines", *J. Struct. Eng.*, **128**(4), 526-532.
- Curtis, L.E. (2004), "Zemmouri- ALGERIA: MW 6.8 earthquake of May 21, 2003", Ed. C.L. Edwards, Technical Council on Lifeline Earthquake Engineering-ASCE, N°27.
- Donaire-Ávila, J., Mollaioli, F., Lucchini, A. and Benavent-Climent, A. (2015), "Intensity measures for the seismic response prediction of mid-rise buildings with hysteretic dampers", *Eng. Struct.*, **102**, 278-295.
- Fakharifar, M., Chen, G., Dalvand, A. and Shamsabadi, A. (2015), "Collapse vulnerability and fragility analysis of substandard RC bridges rehabilitated with different repair jackets under post-mainshock cascading events", *Int. J. Concrete Struct. Mater.*, **9**(3), 345-367.
- Fakharifar, M., Chen, G., Sneed, L. and Dalvand, A. (2015b), "Seismic performance of post-mainshock FRP/steel repaired RC bridge columns subjected to aftershocks", *Compos. Part B*, **72**, 183-198.
- FEMA (2000), Recommended Seismic Design Criteria for New Steel Moment Frame Buildings, FEMA 350, Federal Emergency Management Agency, Washington, DC.
- FEMA (2003), HAZUS-MH Software, Federal Emergency Management Agency, Washington DC.
- Filippou, F.C., Popov, E.P. and Bertero, V.V. (1983), "Effects of bond deterioration on hysteretic behavior of reinforced concrete joints", Report EERC 83-19, Earthquake Engineering Research Center, University of California, Berkeley.
- Gardoni, P., Der Kiureghian, A. and Mosalam, K.M. (2002), "Probabilistic capacity models and fragility estimates for

- reinforced concrete columns based on experimental observations”, *J. Eng. Mech.*, **128**(10), 1024-1038.
- Gardoni, P., Mosalam, K.M. and Der Kiureghian, A. (2003), “Probabilistic seismic demand models and fragility estimates for RC bridges”, *J. Earthq. Eng.*, **7**, 79-106.
- Ghobarah, A. (2001), “Performance-based design in earthquake engineering: state of development”, *Eng. Struct.*, **23**(8), 878-884.
- Housner, G.W. (1963), “The behaviour of inverted pendulum structure during earthquake”, *Bull. Seismol. Soc. Am.*, **53**, 403-417.
- Hwang, H., Jernigan, J.B. and Lin, Y.W. (2000), “Evaluation of seismic damage to Memphis bridges and highway systems”, *J. Bridge Eng.*, **5**(4), 322-330.
- Karamlou, A. and Bocchini, P. (2015), “Computation of bridge seismic fragility by large-scale simulation for probabilistic resilience analysis”, *Earthq. Eng. Struct. Dyn.*, **44**(12), 1959-1978.
- Kehila, F., Remki, R. and Kibboua, A. (2017), “Seismic assessment of Algerian Bridge”, Eds. Rodrigues H., Elnashai A., Calvi G., Facing the Challenges in Structural Engineering, GeoMEast 2017, Sustainable Civil Infrastructures, Springer, Cham.
- Kibboua, A., Naili, M., Benouar, D. and Kehila, F. (2011), “Analytical fragility curves for typical algerian reinforced concrete bridge piers”, *Struct. Eng. Mech.*, **39**(3), 411-425.
- Kim, S.H. and Shinozuka, M. (2004), “Development of fragility curves of bridges retrofitted by column jacketing”, *Prob. Eng. Mech.*, **19**(1), 105-112.
- Liu, M., Lu, B. and Liu, B. (2012), “Study on performance index of reinforced concrete bridge column”, *Adv. Intel. Soft Comput.*, **114**, 189-198.
- Luco, N. and Cornell, C.A. (1998), “Effects of random connection fractures on the demands and reliability for a three-story pre-Northridge (SMRP) structure”, *Proceedings of the 6th US National Conference on Earthquake Engineering*, Earthquake Engineering Research Institute, Oakland, California, May-June.
- Mackie, K.R. and Stojadinović, B. (2004), “Fragility curves for reinforced concrete highway overpass bridges”, *13th World Conference on Earthquake Engineering*, Paper No. 1553, 1-6 August, Vancouver, B.C., Canada.
- Mander, J.B., Priestley, M.J.N. and Park, R. (1988), “Theoretical stress strain model for confined concrete”, *J. Struct. Eng.*, **114**(8), 1804-1826.
- Marra, AM., Salvatori, L., Spinelli, P. and Bartoli, G. (2017), “Incremental dynamic and nonlinear static analyses for seismic assessment of medieval masonry towers”, *J. Perform. Constr. Facil.*, **31**(4), 04017032.
- Mehani, Y., Benouar, D., Bechtoula, H. and Kibboua, A. (2011), “Vulnerability evaluation of the strategic buildings in Algiers (Algeria): a methodology”, *Nat. Hazard.*, **59**(1), 529-551.
- Menegotto, M. and Pinto, P.E. (1973), “Method of analysis for cyclically loaded R.C. plane frames including changes in geometry and nonelastic behaviour of elements under combined normal force and bending”, *Symposium on the Resistance and Ultimate Deformability of Structures Acted on By Well-Defined Repeated Loads*, International Association for Bridge and Structural Engineering, Zurich, Switzerland, 15-22.
- Moschonas, I.F., Kappos, A.J., Panetsos, P., Papadopoulos, V., Makarios, T. and Thanopoulos, P. (2009), “Seismic fragility curves for greek bridges: methodology and case studies”, *Bull. Earthq. Eng.*, **7**(2), 439-468.
- Mosleh, A., Razzaghi, M.S., Jara, J. and Varum, H. (2016), “Development of fragility curves for RC bridges subjected to reverse and strike-slip seismic sources”, *Earthq. Struct.*, **11**(3), 517-538.
- Nielson, B.G. and DesRoches, R. (2007a), “Analytical seismic fragility curves for typical bridges in the Central and Southeastern United States”, *Earthq. Spectra*, **23**(3), 615-633.
- Paulay, T. and Priestley, M.N.J. (1992), *Seismic Design of Reinforced Concrete and Masonry Buildings*, Wiley-Interscience, New York.
- PEER Ground Motion Database (2013), Pacific Earthquake Engineering Research Center (PEER), from: <http://ngawest2.berkeley.edu/>
- Priestley, M.J.N., Calvi, G.M. and Kowalsky, M.J. (2007), *Direct Displacement-Based Seismic Design of Structures*, IUSS Press, Pavia, Italy.
- Priestley, M.J.N., Seible, F. and Calvi, G.M. (1996), *Seismic Design and Retrofit of Bridges*, Wiley, New York.
- Ramanathan, K., DesRoches, R. and Padgett, J.E. (2012), “A comparison of pre- and post-seismic design considerations in moderate seismic zones through the fragility assessment of multi span bridge classes”, *Eng. Struct.*, **45**, 559-573.
- Remki, M., kehila, F., Bechtoula, H. and Bourzam, A. (2016), “Seismic vulnerability assessment of composite reinforced concrete-masonry building”, *Earthq. Struct.*, **11**(2), 371-386.
- RPOA (2008), Algerian Seismic Regulation Code for Bridge Structures, Document Technique Règlementaire, Ministère des Travaux Publics, Algiers, Algeria.
- SeismoMatch (2016), Seismosoft Earthquake Engineering Software Solutions, <http://www.seismosoft.com>.
- SeismoStruct (2016), Seismosoft Earthquake Engineering Software Solutions, <http://www.seismosoft.com>.
- Shinozuka, M., Feng, M.Q., Kim, H., Uzawa, T. and Ueda, T. (2003), “Statistical analysis of fragility curves”, MCEER Report-03-0002.
- Stefanidou, S.P. and Kappos, A.J. (2017), “Methodology for the development of bridge-specific fragility curves”, *Earthq. Eng. Struct. Dyn.*, **46**(1), 73-93.
- Takemura, H. and Kawashima, K.X. (1997), “Effect of loading hysteresis on ductility capacity of reinforced concrete bridge piers”, *J. Struct. Eng.*, **43A**, 849-858.
- Tavares, D.H., Padgett, J.E. and Paultre, P. (2012), “Fragility curves of typical as-built highway bridges in eastern Canada”, *Eng. Struct.*, **40**, 107-118.
- Vamvatsikos, D. and Cornell, C.A. (2002), “Incremental dynamic analysis”, *Earthq. Eng. Struct. Dyn.*, **31**(3), 491-514.
- Zhang, Y., Fan, J. and Fan, W. (2016), “Seismic fragility analysis of concrete bridge piers reinforced by steel fibers”, *Adv. Struct. Eng.*, **19**(5), 837-848.
- Zhong, J., Pang, Y., Jeon, J.S., DesRoches, R. and Yuan, W. (2016), “Seismic fragility assessment of long-span cable-stayed bridges in China”, *Adv. Struct. Eng.*, **19**(11), 1797-1812.

AT